Photoelectron spectroscopy of cold aluminum cluster anions: Comparison with density functional theory results

Lei Ma,[1,2] Bernd v. Issendorff,[2,a)] and Andrés Aguado[3,b)]
[1]*Department of Physics, Nanjing University, 210093 Nanjing,China*
[2]*Fakultät für Physik, Universität Freiburg, H.Herderstr. 3, D- 79104 Freiburg, Germany*
[3]*Departamento de Física Teórica, Universidad de Valladolid, Valladolid 47011, Spain*

(Received 15 December 2009; accepted 9 February 2010; published online 8 March 2010)

Photoelectron spectra of cold aluminum cluster anions Al_n^- have been measured in the size range $n=13-75$ and are compared to the results of density functional theory calculations. Good agreement between the measured spectra and the calculated density of states is obtained for most sizes, which gives strong evidence that the correct structures have been found. In particular the results confirm the occurrence of rather different structural motifs in this size range, from fcc-like stacks over fragments of decahedrons to disordered structures. An analysis of the density of states of representatives of the different structural motifs shows that the electronic structure is strongly influenced by the cluster geometry, and that a clear jelliumlike electron shell structure is present only in some exceptional cases. © *2010 American Institute of Physics*. [doi:10.1063/1.3352445]

I. INTRODUCTION

Aluminum is an interesting material. Being an s-p metal, its electronic system is essentially free electronlike, but still significantly more complex than that of the monovalent alkaline metals. In the trivalent aluminum the Fermi-surface extends into the third Brillouin zone,[1] which causes a distinct perturbation of the electron dispersion at the zone boundaries.[2] This is the reason why the density of states (DOS) significantly deviates from a simple square root function at certain energies.[3] The perturbation of free electron behavior is even more pronounced for clusters. Due to the atomic $3s^2\,3p^1$ configuration of aluminum, in small clusters a fully occupied s-band and a partly filled p-band are formed, which are separated by a bandgap.[4] With increasing cluster size both bands broaden; eventually they overlap. This facilitates the hybridization between s- and p-states and increases the free electron character of the states. The question, therefore, arises at what size (if at all) the clusters exhibit an electronic DOS similar to that of an ideal free electron particle, that is of an structureless jellium sphere.[5,6] Experiments have demonstrated the strong influence of the s-p separation especially for small sizes. The ionization potentials of very small clusters (up to about size $n=6$), for example, increase with cluster size;[4] this is very unusual for metal clusters, but can be easily understood as an effect of the broadening of the partly occupied p-band.[7] A careful comparison of the photoelectron spectra of aluminum and gallium clusters showed that the separation of s- and p-derived bands persists at least up to size $n=8$.[8,9] In measurements of the ionization potentials of larger clusters steps in the size dependence of the ionization potentials were observed, which are partly in agreement with jellium model predictions, but not consistently.[4] Measurements of the polarizability of aluminum clusters indicated that simple metal behavior develops only at sizes larger than about $n=40$.[10] In mobility measurements some influence of the electronic shell structure onto the cluster shapes was seen in the size range $n=5-72$, but also a more complex behavior than one would expect from simple deformable jellium model predictions.[11] Photoelectron spectroscopy (PES) on larger cold Al_n^- with $n=3-32$ (Ref. 12) and $n=2-162$ (Ref. 13) showed some features which can be seen in agreement with an electron shell filling pattern; nevertheless, the structures were much less clear than in the PES results of simple systems such as, e.g., sodium clusters.[14,15] In mass spectra of large clusters which were photoionized close to the threshold, an interesting interplay between geometrical and electronic structure was observed.[16] While cold clusters seem to be strongly influenced by the geometrical structure, and exhibit features in agreement with an octahedral atomic packing scheme,[17] warm clusters exhibit electronic shell effects up to sizes of at least $n=700$. Finally, also the melting points of aluminum clusters, at least in the size range $n=35$ to 70, are influenced by an interplay of structural and geometric effects.[18]

All this demonstrates that aluminum clusters have an electronic system which is rather strongly perturbed by the interaction with the atomic lattice. In order to understand the properties of aluminum clusters, it is therefore indispensable to know their geometric structure. While the structure of very small sizes has been known for a long time,[19,20] the treatment of larger sizes with *ab initio* methods became possible only recently.[18,21–27] The results generally are in good agreement with measurements of the size dependence of binding energies[18,23] and cluster mobilities.[26] A comparison with spectroscopic measurements, however, has not been done yet, except for the pioneering PES/density functional theory (DFT) study of Akola *et al.* on ten different sizes between $n=12$ and $n=55$.[28,29]

a)Electronic mail: bernd.von.issendorff@uni-freiburg.de.
b)Electronic mail: aguado@metodos.fam.cie.uva.es.

This was the motivation for the work presented here. In the following, we will briefly describe the experiment and the theoretical methods. Then we will present the results and discuss them especially with respect to the effects of the electron-lattice interaction.

II. EXPERIMENTAL METHODS

Aluminum clusters are produced in a magnetron gas aggregation cluster source. Aluminum is sputtered from a 2 in. magnetron into a mixture of helium and argon (roughly 3:1) with a total pressure of about 0.5 mbar inside a liquid nitrogen cooled tube, where it condenses to particles. The high density of charge carriers produced by the magnetron discharge leads to an efficient charging of the clusters (both anions and cations are formed). The buffer gas with the clusters expands through an adjustable iris aperture into the vacuum. The clusters enter a radio-frequency (RF) octupole, which guides the anions into the next chamber, where they are trapped in a RF 12-pole trap[30] attached to a coldhead. In the trap, which is cooled to 80 K, the clusters are thermalized by collisions with helium buffer gas with a pressure of about 10^{-3} mbar. Although the trap can be cooled to 10 K, it was more convenient to work at 80 K: at 10 K argon freezes out inside the trap, which can lead to charging problems. The photoelectron spectra are practically identical at the two temperatures. Bunches of cluster ions are extracted from the trap and inserted into a high resolution, double reflectron time-of-flight mass spectrometer, where a multiwire mass gate positioned at the focus point of the first reflector can be used to select clusters of a certain mass with a resolution of about $m/dm=2000$. The size selected clusters get reflected (and rebunched) by the second reflector, are decelerated by a pulsed electric field and enter the interaction region of a magnetic bottle time-of-flight photoelectron spectrometer, where they are irradiated by a laser pulse from a KrF excimer laser. Typically, photoelectron spectra are averaged over 30 000 laser shots at a repetition rate of 100 Hz. The spectrometer is calibrated by measuring the known photoelectron spectrum of Pt^-, which leads to an error of the measured binding energies of less than 30 meV.

III. COMPUTATIONAL METHODS

Calculations were performed at the Kohn–Sham density functional theory[31] level. We employ the SIESTA code,[32] with exchange and correlation effects treated within the spin-polarized generalized gradient approximation in its PBE implementation,[33] and norm-conserving pseudopotentials to describe the core electrons.[34,35] The basis set employed to expand the cluster wave function contains five basis functions per Al atom (a double zeta plus polarization basis in standard notation[32]). The spatial extension of the basis functions is determined by an energy shift[32] of 20 meV. The fast-Fourier-transform mesh employed to evaluate some terms in the Hamiltonian is determined by a mesh cutoff[32] of 100 Ryd. The accuracy obtained by these settings has been tested in our previous works on aluminum clusters.[18,21,23,26] In these reports we also provide a description of the computational strategy employed in the search for the putative global minimum (GM) structures.

The putative GM structures for Al_n^- cluster anions with $n=13-70$ atoms have been reported in two recent works.[18,26] In the small size range containing $n=13-34$ atoms,[26] we could only provide an indirect confirmation of the anion structures by comparing the DFT cluster stabilities with available abundance mass spectra.[36] In the large size range containing $n=35-70$ atoms,[18] we showed an explicit comparison between DFT and experimental cohesive energies in an attempt to confirm the accuracy of the DFT anion structures. The experimental cohesive energies for the solid clusters are obtained from the dissociation energies of the liquid-like clusters and the latent heats for melting.[18] Most clusters with less than 34 atoms show a very broad heat capacity melting peak, which prevents an accurate determination of the latent heats and hence of the solid cohesive energies. This is why the explicit comparison of theoretical and experimental cohesive energies could not be carried out for the small cluster sizes.

The main goal of this paper is to provide an additional, and more explicit, confirmation of the proposed anion structures by comparing the electronic DOS of the putative global minima with the PES results. The photoelectron spectra provide a much more sensitive structural fingerprint than the cohesive energies alone. Also, the vertical detachment energies (VDEs) have been calculated and compared to the corresponding experimental values obtained from an analysis of the photoelectron spectra for $n=13-75$. The cluster structures for $n=71-75$ are obtained here for the first time. We have also found a more stable isomer for Al_{23}^-, as compared to our previous work[26] (see next section for details).

The VDEs were calculated through a $\Delta-$SCF calculation, that is, as the total energy difference between the anion and the neutral cluster, both clusters adopting the geometry of the anion. In order to simulate the experimental photoelectron spectra, we have broadened each line of the KS eigenvalue spectrum by a Gaussian function of width 0.10–0.13 eV (different widths were used for different clusters sizes; for a good agreement with the measured spectra the smaller clusters in general required a slightly stronger broadening then the larger ones, probably indicating a stronger influence of vibrational excitations in the former). The calculated DOS was then globally shifted in order to align the binding energy of the highest occupied orbital (HOMO) with the theoretical VDE value. After this data processing, the theoretical DOS are still systematically shifted by 0.1 eV to lower energies as compared to the PES results, that is, we have a systematic error of 0.1 eV in the VDE values, which we consider to be well within the expected accuracy of the DFT methodology (and of the PES). The DOS and theoretical VDE values shown in the next section include this additional 0.1 eV shift, just in order to facilitate the visual comparison.

IV. RESULTS

The measured photoelectron spectra for the cluster sizes $n=13-75$ are shown together with the calculated DOS of the putative GM structures in Fig. 1. The photoelectron spectra

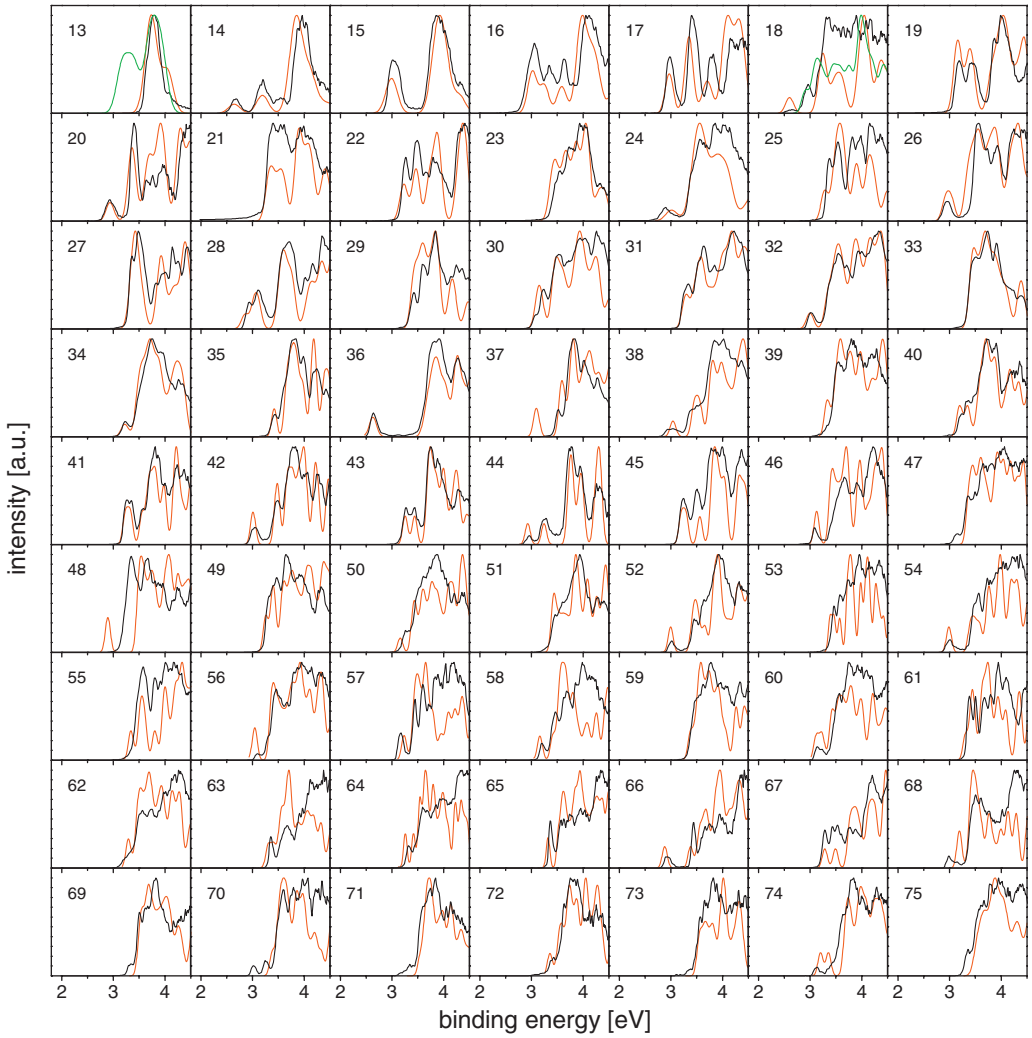

FIG. 1. Photoelectron spectra of cold (T=80 K) aluminum cluster anions, measured at a photon energy of 4.99 eV (thick dark lines), in comparison with the electron DOS as calculated for the lowest energy structure found (thin red/light lines). For size $n=13$, the thin green (light) curve shows the DOS obtained from a decahedral isomer. For $n=18$, we show the DOS curves for two nearly degenerate isomers.

are very similar to those obtained by Wang and co-workers.[13] The only difference is that the resolution of our spectra is slightly better due to the lower cluster temperature; furthermore, the relative peak heights in the spectra sometimes are different because of the different photon energy used.

As already discussed by Li *et al.*,[13] in the spectra for certain sizes small peaks at low binding energies appear which indicate the opening of a new electron shell. In some cases the sizes where this occurs are in good agreement with spherical jellium calculations, which usually predict major shell closings to appear at 20, 34, 40, 58, 92, 138, and 198 electrons. As aluminum is trivalent, in clusters where a new shell occurs this shell can be occupied by one to three electrons. This is the case for Al_n^- with $n=14$ (40+3 electrons), $n=20(58+3)$, $n=46(138+1)$ or $n=66(198+1)$. No new shell, however, is observed for Al_{31}^- (92+2 electrons). Other sizes exhibit similar bandgaps between the uppermost and lower lying states, but are not in agreement with the simple jellium model predictions, such as $n=26$, 36, 44, 52, and 54. So obviously in the aluminum clusters the DOS is rather strongly influenced by the interaction of the electrons with the ionic background. This makes it possible to use the PES results as a fingerprint of the geometrical structure of the cluster. Indeed the calculated DOS for most sizes is in good agreement with the measured spectra, which gives strong evidence that the correct structure has been found.

The geometrical structures for $n=13-34$ and $n=35-70$ have been shown, respectively, in Refs. 18 and 26; the coordinate files of all cluster sizes treated in this report are available in Refs. 37 and 38.

For the sizes $n=13-15$ the results of Akola *et al.*[28] are reproduced. In particular we find the same assignment for Al_{13}^-: in Fig. 1 the measured spectrum is compared to the DOS of the GM structure (a perfect icosahedron) and to the DOS of a low lying isomer, namely a perfect decahedron. Very clearly, only the DOS of the icosahedron fits the measured spectra. All the structures with $n=14-20$ are obtained by adding atoms onto the surface of this 13-atom icosahedron.[26] Sizes 16 and 17 have the same structure as found for neutral aluminum clusters by Chuang *et al.*[22] For size 18 the spectrum is not well resolved; here theory predicts several isomers almost degenerate with the GM, so most probably more than one isomer is present in the experiment. Sizes $n=21-23$ are based on fcc-like atomic packing,

but with substantial shape distortions.[26] In particular, for sizes 19, 20, and 23 we find the same structures as Akola *et al.*[28] (we were not able to locate Akola's GM structure for Al_{23}^- in our previous work, but here we found that it is 0.08 eV more stable than our previous putative GM. Only this new structure leads to a good DOS/PES agreement).

For larger sizes, the ranges $n=26-29$, $n=31-36$, $n=40-45$, $n=52$, $n=61-66$, and $n=72$ show good to very good agreement between DOS and PES results; here again most probably the correct geometries have been found. This gives strong evidence that some new structural motifs we recently proposed[18,26] are correct. For sizes $n=24-26$, the GM structures are obtained by adding atoms onto the surface of a perfect 23-atom decahedron. For Al_{28}^-, we confirm a closed packed double-tetrahedron structure[25,26] based on fcc packing. Al_{36}^- has a novel closed packed structure, which is a distorted fragment of a 54-atom decahedron,[23] and has an outer shape close to a tetrahedron. Al_{44}^- is a closed packed structure as well, a fcc stack with a stacking fault and D_{3h} symmetry.[18] Al_{66}^- has a rather disordered structure, but a close to perfectly spherical shape. For Al_{52}^- and Al_{54}^- the agreement is not as good, but probably they have an almost closed packed structure with a tetrahedral shape again.

For some sizes such as $n=37$, 47–48, 50, 56, 68–71, and 74, it is clear that the DFT calculations were not able to locate the GM structure. Al_{37}^-, for example, is obtained by adding one atom onto the surface of Al_{36}^-, which is a geometric shell closing. The DOS associated with this structure shows a low energy peak which is absent from the experimental photoelectron spectra. We have tried to locate a more stable structure by means of simulated annealing runs, and also of selective quenching from high-temperature molecular dynamics trajectories, but all attempts were unsuccessful. It is at least reassuring to see that we also got a bad agreement between theoretical and experimental cohesive energies for these sizes,[18] which therefore deserve further consideration. For most other sizes not explicitly mentioned, the DOS/PES agreement is reasonable, although not perfect. These remaining sizes have less structured spectra, and are always associated with the presence of low-lying local minima in the DFT calculations, so that several isomers might contribute to the spectra. We are therefore confident that the located structures are reasonable.

The experimental VDE values have been extracted from an analysis of the photoemission spectra, and are compared to the corresponding theoretical values in Fig. 2. The agreement between theory and experiment is very good, except for those sizes where the GM search failed. Note that the theoretical results reproduce very well the measured size dependence of the amplitude of the odd-even oscillation—while in some size ranges the VDE changes by more than 0.5 eV from size to size, there are other ranges where the oscillation is almost negligible.

Having identified the geometries of the majority of the clusters, we can now make use of the theoretical results to analyze their electronic structure in detail. This will be done in the next section.

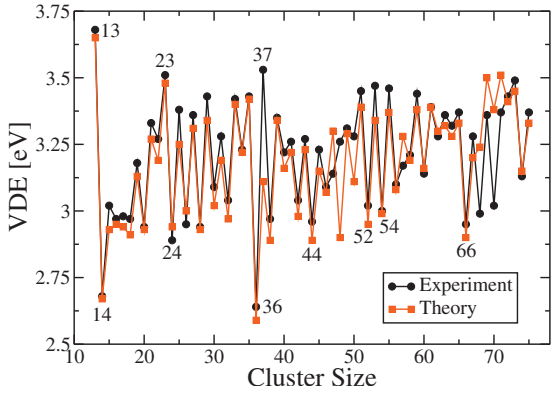

FIG. 2. The VDE of Al_n^- cluster anions is shown as a function of cluster size. The filled black points are the experimental results, and the filled red (light) squares the theoretical results. The DFT results have been globally shifted by 0.1 eV (the systematic error) in order to help the comparison.

V. DISCUSSION AND INTERPRETATION OF THE RESULTS

We first look at the atomic orbital character of the electronic wave functions in the studied size range. In Fig. 3 we show the total and the partial DOS for three cluster sizes, as well as for the bulk. Obviously even already in Al_{13}^- the hybridization between atomic s- and p-orbitals is close to that of the bulk; no reminiscence of separated s- and p-bands can be seen here anymore. The same result was obtained by Cheng *et al.*,[39] and supports the statement by Upton[40] that s- and p-bands merge for sizes slightly larger than $n=6$. For sizes $n=28$ and $n=66$ the partial DOS are even closer to that of the bulk. This demonstrates that although the DOS is strongly influenced by the cluster structure, the general hybridization between atomic s- and p-states is not. Another observation can be immediately made: the total width of the cluster valence band rapidly converges to the bulk value. Although in Al_{13}^- there is just 1 internal atom and 12 surface atoms, the total bandwidth is already 80% of the bulk value; for Al_{28}^- it is even 90%.

In Fig. 4 the DOS of four special sizes ($n=36$, 44, 54,

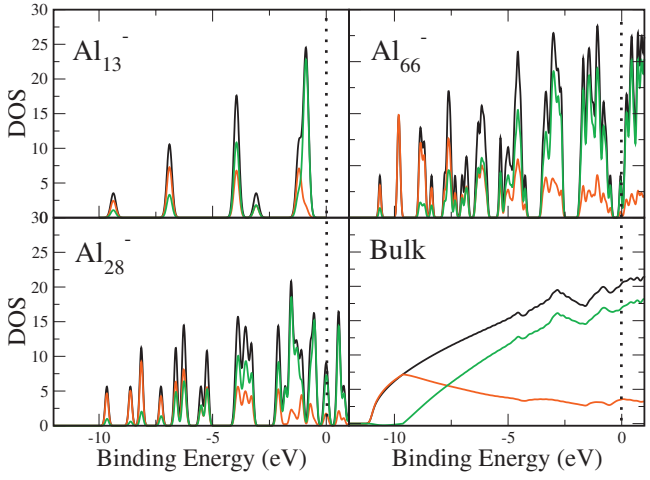

FIG. 3. The calculated total electron DOS of Al_n^- clusters and the bulk are shown by the black lines. The red and green lines indicate the partial contributions from atomic s- and p- states. The Fermi energy, shown by the dotted vertical lines, is taken as the energy reference.

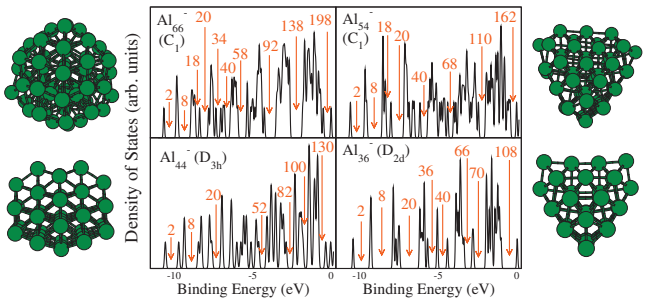

FIG. 4. Total DOS of four cluster sizes (Al_{36}^-, Al_{44}^-, Al_{54}^-, and Al_{66}^-), which exhibit a large bandgap in the photoelectron spectra. The geometrical structure of the clusters is indicated.

and 66) are shown. For all of them, the photoelectron spectrum exhibits a single peak at the threshold, which is clearly separated from the rest of the spectrum. This shows that the corresponding neutral cluster has a closed shell electronic structure. But each of them has a different structural motif: $n=36$ and 44 are geometrical shell closings with distorted decahedral and fcc stacking, respectively; $n=54$ has a similar packing as $n=36$ but it is not a geometrical shell closing; finally, $n=66$ has a more disordered structure based on polytetrahedral packing with a spherical outer shape. Only for size $n=66$ the DOS is in agreement with the predictions of the spherical jellium model (SJM), which predicts a shell closure for 198 electrons. Indeed the DOS of Al_{66}^- exhibits an electronic shell system in perfect agreement with the SJM; large gaps appear in the DOS for cumulative electron numbers 8, 18, 20, 34, 40, 58, 92, 138, and 198. This is obviously a consequence of the close to perfectly spherical shape of this cluster. The other sizes have more crystalline structures which deviate strongly from a spherical shape; consequently their DOS is significantly perturbed. Al_{44}^- exhibits gaps in the DOS for 20, 26, 52, 82, 100, and 130 electrons, which clearly deviates from the SJM predictions. Al_{36}^- also has a well structured DOS, as a result of a well defined symmetry (D_{2d}, but close to D_{4h}), and exhibits clear gaps at 20, 36, 40, 66, 70, and 108 electrons. The gaps are not as well defined in the less perfect Al_{54}^- structure; they occur for 20, 40, 68, 110, and 162 electrons. Only for the innermost peaks of Al_{36}^- and Al_{44}^- (up to the gap for 20 electrons, approximately) were we able to identify the expected splittings of jelliumlike levels into sublevels with the appropriate (D_{3h} or D_{2d}) point-group symmetry. For lower binding energies, it is not possible anymore to understand the level structure as the result of applying a small perturbation with the lattice point-group symmetry to the SJM levels. Here specific electron shell closings become unpredictable.

This shows that aluminum clusters have an electronic system which only in special cases (for close to spherical geometries) exhibits an electron shell structure in accordance with the SJM; for most sizes the shell structure is perturbed beyond recognition. This explains immediately why electron shell effects could only be observed for hot, liquid aluminum clusters: these can be expected to adopt, in an average sense, spherical disordered structures such as Al_{66}^-. Most cold clusters adopt instead more crystalline, faceted shapes, which destroy the usual electron shell structure.

The strong electron-lattice interaction is also responsible for the complex size dependence of the VDE shown in Fig. 2. The amplitude of the odd-even oscillations observed is often larger than 0.5 eV. As the average level spacing at the Fermi energy in an aluminum cluster with around 50 atoms is only about $4E_F/3N_e=0.25$ eV,[41] such a large amplitude can only be explained by strong Jahn–Teller-deformation of the clusters or even complete structural changes induced by the electronic system. Obviously some of the structural motifs are more susceptible to this electronic influences then others, which is the reason why the amplitude of the odd-even-oscillation is very different in different size ranges.

VI. CONCLUSIONS

Well resolved photoelectron spectra of cold aluminum cluster anions have been compared to the DOS of putative GM structures obtained by DFT methods. A number of new cluster structure motifs could be identified and confirmed. This allows a reliable analysis of the electronic properties of the clusters. A few sizes exhibit an electron shell structure in accordance with a simple SJM. For most sizes, however, there is no resemblance at all to the DOS of a spherical particle. This demonstrates that here a classification of the electron wave functions in terms of angular momentum eigenstates is not justified.

ACKNOWLEDGMENTS

We gratefully acknowledge the support of the Deutsche Forschungsgemeinschaft, the Spanish "Ministerio de Ciencia e Innovación," the European Regional Development Fund, and "Junta de Castilla y León" (Project Nos. FIS2008-02490/FIS and GR120).

[1] N. W. Ashcroft and N. D. Mermin, *Solid State Physics* (Saunders College, Philadelphia, 1976).
[2] H. J. Levinson, F. Greuter, and E. W. Plummer, Phys. Rev. B **27**, 727 (1983).
[3] N. W. Ashcroft, Phys. Rev. B **19**, 4906 (1979).
[4] K. E. Schriver, J. L. Persson, E. C. Honea, and R. L. Whetten, Phys. Rev. Lett. **64**, 2539 (1990).
[5] J. Martins, R. Car, and J. Buttet, Surf. Sci. **106**, 265 (1981).
[6] W. Ekardt, Phys. Rev. B **29**, 1558 (1984).
[7] T. H. Upton, Phys. Rev. Lett. **56**, 2168 (1986).
[8] G. Ganteför and W. Eberhardt, Chem. Phys. Lett. **217**, 600 (1994).
[9] C.-Y. Cha, G. Ganteför, and W. Eberhardt, J. Chem. Phys. **100**, 995 (1994).
[10] W. A. de Heer, P. Milani, and A. Châtelain, Phys. Rev. Lett. **63**, 2834 (1989).
[11] M. F. Jarrold and J. E. Bower, J. Chem. Phys. **98**, 2399 (1993).
[12] K. J. Taylor, C. L. Pettiette, M. J. Craycraft, O. Chesnovsky, and R. E. Smalley, Chem. Phys. Lett. **152**, 347 (1988).
[13] X. Li, H. Wu, X. B. Wang, and L. S. Wang, Phys. Rev. Lett. **81**, 1909 (1998).
[14] G. Wrigge, M. A. Hoffmann, and B. v. Issendorff, Phys. Rev. A **65**, 063201 (2002).
[15] O. Kostko, B. Huber, M. Moseler, and B. v. Issendorff, Phys. Rev. Lett. **98**, 043401 (2007).
[16] B. Baguenard, M. Pellarin, J. Lermé, J. L. Vialle, and M. Broyer, J. Chem. Phys. **100**, 754 (1994).
[17] T. P. Martin, U. Näher, and H. Schaber, Chem. Phys. Lett. **199**, 470 (1992).
[18] A. K. Starace, C. M. Neal, B. Cao, M. F. Jarrold, A. Aguado, and J. M. López, J. Chem. Phys. **131**, 044307 (2009).
[19] R. O. Jones, J. Chem. Phys. **99**, 1194 (1993).
[20] B. K. Rao and P. Jena, J. Chem. Phys. **111**, 1890 (1999).

[21] A. Aguado and J. M. López, J. Phys. Chem. B **110**, 14020 (2006).
[22] F.-C. Chuang, C. Z. Wang, and K. H. Ho, Phys. Rev. B **73**, 125431 (2006).
[23] A. K. Starace, C. M. Neal, B. Cao, M. F. Jarrold, A. Aguado, and J. M. López, J. Chem. Phys. **129**, 144702 (2008).
[24] J. Sun, W.-C. Lu, Z.-S. Li, C.-Z. Wang, and K. M. Ho, J. Chem. Phys. **129**, 014707 (2008).
[25] W. Zhang, W.-C. Lu, J. Sun, C. Z. Wang, and K. M. Ho, Chem. Phys. Lett. **455**, 232 (2008).
[26] A. Aguado and J. M. López, J. Chem. Phys. **130**, 064704 (2009).
[27] W. Zhang, W.-C. Lu, Q.-J. Zang, C. Z. Wang, and K. M. Ho, J. Chem. Phys. **130**, 144701 (2009).
[28] J. Akola, M. Manninen, H. Häkkinen, U. Landman, X. Li, and L.-S. Wang, Phys. Rev. B **60**, R11297 (1999).
[29] J. Akola, M. Manninen, H. Häkkinen, U. Landman, X. Li, and L.-S. Wang, Phys. Rev. B **62**, 13216 (2000).
[30] D. Gerlich, Adv. Chem. Phys. **82**, 1 (1992).
[31] W. Kohn and L. J. Sham, Phys. Rev. **140**, A1133 (1965).
[32] J. M. Soler, E. Artacho, J. D. Gale, A. Garcia, J. Junquera, P. Ordejón, and D. Sánchez-Portal, J. Phys.: Condens. Matter **14**, 2745 (2002).
[33] J. P. Perdew, K. Burke, and M. Ernzerhof, Phys. Rev. Lett. **77**, 3865 (1996).
[34] D. R. Hamann, M. Schlüter, and C. Chiang, Phys. Rev. Lett. **43**, 1494 (1979).
[35] L. Kleinman and D. M. Bylander, Phys. Rev. Lett. **48**, 1425 (1982).
[36] R. L. Hettich, J. Am. Chem. Soc. **111**, 8582 (1989).
[37] See supplementary material at http://dx.doi.org/10.1063/1.3352445 for the coordinate files.
[38] Web page of the "Nanometric Properties of Matter" research group (http://metodos.fam.cie.uva.es/GIR).
[39] H. Cheng, R. S. Berry, and R. L. Whetten, Phys. Rev. B **43**, 10647 (1991).
[40] T. H. Upton, J. Chem. Phys. **86**, 7054 (1987).
[41] R. Kubo, J. Phys. Soc. Jpn. **17**, 975 (1962).